

Synthesis and Characterization of Poly(ester amides) with a Variable Ratio of Branched Odd Diamide Units

Sara K. Murase, Lourdes Franco, Luís J. del Valle, Jordi Puiggali

Departament d'Enginyeria Química, Universitat Politècnica de Catalunya, Av. Diagonal 647, Barcelona E-08028, Spain

Correspondence to: J. Puiggali (E-mail: jordi.puiggali@upc.es)

ABSTRACT: The synthesis of a series of poly(ester amide)s constituted by glycolic acid, adipic acid, and different ratios of 1,3-pentanediamine and 1,5-pentanediamine units was studied and the derived copolymers were characterized. Thermal polycondensation between the potassium adipate salt and the appropriate ratio of *N,N'*-bis(chloroacetyl)-1,3-pentanediamine and *N,N'*-bis(chloroacetyl)-1,5-pentanediamine was proved to be effective, proceeded with high yield, and rendered samples with moderate molecular weight for carefully controlled competitive thermal degradation reactions. Physical properties were highly dependent on the final composition. In particular, crystallinity and thermal stability decreased with 1,3-pentanediamine unit content, that is, with the incorporation of lateral ethyl groups into the main chain. The presence of these units also changed solubility in solvents like methanol and degradability in a protease K enzymatic medium. Specifically, incorporation of 1,3-pentanediamine units led to a gradual increase in degradability. All poly(ester amide)s were able to establish intermolecular hydrogen bonding interactions, which in semicrystalline samples pointed to typical sheet structures of polyamides according to X-ray diffraction and infrared spectroscopic data. © 2013 Wiley Periodicals, Inc. *J. Appl. Polym. Sci.* **2014**, *131*, 40102.

KEYWORDS: biodegradable; degradation; polycondensation

Received 22 July 2013; accepted 22 October 2013

DOI: 10.1002/app.40102

INTRODUCTION

Poly(ester amide)s (PEAs) constitute a peculiar family of biodegradable polymers due to the presence of both ester and amide groups, which ensures degradability and to some improved properties compared with related polyesters.^{1–3} A great effort has been made in the development of PEAs since the preparation of the first derivatives in the 1970s.⁴ Different synthesis methodologies have been successfully applied (e.g., ring-opening polymerization and polycondensation including melt, interfacial, and solution polymerization) to obtain polymers with highly variable structural units and chain architecture. Amorphous, semicrystalline, elastomeric, and functionalized materials can be easily prepared by selecting the appropriate synthesis strategy and components. Thus, a large number of applications have been found for biodegradable PEAs, especially in the biomedical field, such as microspheres and coatings for drug delivery,^{5–8} hydrogels,^{9,10} smart materials,¹¹ thermosensitive polymers,¹² nanocomposites,^{13–15} and adhesives.¹⁶ This family is extremely complex since different dispositions of amide and ester groups can be considered, even for orderly arrangements of monomers. In this sense, it seems interesting to know the characteristics of each type or organi-

zation for the appropriate selection of combinations of building units that allow tuning the properties of the final polymer.

Poly(ester amide)s based on glycolic acid, diamines and dicarboxylic acids have been proposed as bioabsorbable surgical sutures due to their combination of the above properties as well as ability to be sterilized by gamma radiation without serious loss of suture strength.^{17,18} These polymers are defined by the repeat unit $-\text{[OCH}_2\text{CO-NH(CH}_2\text{)}_n\text{NH-COCH}_2\text{O-CO(CH}_2\text{)}_{m-2}\text{CO]}-$ and can be synthesized by both interfacial polymerization of a diamidediol and a diacid chloride^{17,18} and thermal polycondensation involving a dicarboxylic salt and a chloroacetate derivative of a diamine.¹⁹

A series of polymers derived from the even 1,6-hexanediamine and different even dicarboxylic acids (from succinic to dodecanoic acid) were previously synthesized and characterized.^{20,21} Calorimetric data indicated a melting temperature in the 150–115°C range that tended to the fusion temperature of polyethylene as the number of methylene groups increased. Glass transition temperatures were in the 0–30°C range and decreased with methylene content due to greater flexibility of

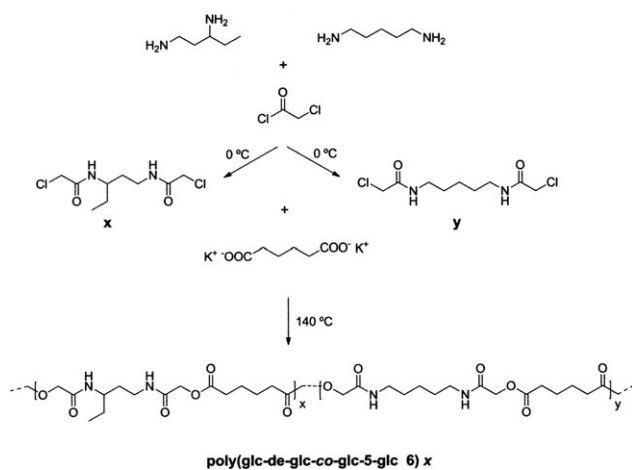


Figure 1. Synthesis scheme for preparation of copolymers from potassium adipate and mixtures of *N,N'*-bis(chloroacetyl)-1,3-pentanediamine and *N,N'*-bis(chloroacetyl)-1,5-pentanediamine.

the molecular chain. It was also demonstrated that the adipic acid derivative was hydrolytically degradable through the cleavage of ester bonds that mainly belonged to the amorphous phases. Furthermore, the polymer was susceptible to enzymatic attack of lipase from *Pseudomonas cepacia* and proteases like proteinase K.

1,3-Pentanediamine (DYTEK® EP) is a low viscous, low odor, biodegradable, liquid diamine featuring an odd number of carbon atoms (i.e., 5), an ethyl side branch, an asymmetric structure, and different amine reactivity (i.e., the terminal amine group is about 100 times more reactive than the ethyl-hindered amine group).²² The monomer can be used to obtain polyamides with low viscosity, crystallinity, and T_g because of the incorporation of ethyl branches. In formulated products, 1,3-pentanediamine derivatives can improve flow, penetration, wetting, or solubility compared with straight chain diamines, and have specific applications as coatings, sealants, and elastomers.

The goal of this work is to get insight into the melt condensation procedure with formation of metal salts to prepare samples derived from odd diamine units and compare their physical properties and biodegradability with those of previously studied samples derived from even units. Furthermore, copolymers with different contents of 1,5-pentanediamine and 1,3-pentanediamine were considered to modulate the degree of crystallinity, glass transition temperature, and biodegradability. It is expected that these novel samples containing 1,3-pentanediamine units may find applications as new biodegradable coatings (e.g., for multifilament bioabsorbable sutures).

The use of 1,5-pentanediamine as raw material is receiving increasing interest because this monomer can be obtained from the amino acid lysine produced from plant materials by fermentation technology.²³ In fact, biobased nylons made from this monomer have recently been commercialized by Ajinomoto Co. and Toray Industries. Specifically, nylon 56 fibers are claimed to have the same strength and heat resistance as conventional nylon fibers made from the petrochemical hexamethylenediamine derivative.²⁴ Several works focus on the peculiar structures of

nylons derived from 1,5-pentanediamine (e.g., nylons 55 and 56), which are characterized by the establishment of intermolecular hydrogen bonds along two different directions.^{25–27}

EXPERIMENTAL

Materials

Reagents (1,3-pentanediamine, 1,5-pentanediamine, adipic acid, and chloroacetyl chloride) and solvents (ethyl ether, potassium hydroxide, methanol, and chloroform) were purchased from Sigma Aldrich and used as received to perform the synthesis in Figure 1.

Enzymes used in the degradation studies (i.e., lipase from *Rhizopus oryzae* and proteinase K from *Tritirachium album*) and Dulbecco's phosphate-buffered saline medium were also purchased from Sigma Aldrich.

Potassium adipate was obtained by neutralization of an aqueous solution of adipic acid (0.3 g/mL) with KOH (4M).

N,N'-Bis(chloroacetyl)-1,3-pentanediamine and *N,N'*-Bis(chloroacetyl)-1,5-pentanediamine

A solution of 8.75 mL (0.11 mol) of chloroacetyl chloride dissolved in 20 mL of diethyl ether was added dropwise to 50 mL of an aqueous solution of 1,3-pentanediamine (6 mL, 0.05 mol) or 1,5-pentanediamine (5 g, 0.05 mol) and NaOH (0.1 mol) placed in a round bottom flask. The resulting two phase mixture was stirred in an ice-cooled bath for 1 h. Drops of a 2M sodium hydroxide solution were also added to keep the pH close to 11 and neutralize the hydrochloric acid produced during reaction. In both cases, a white solid precipitated, which was then washed with water and diethyl ether.

N,N'-Bis(chloroacetyl)-1,3-pentanediamine

Yield: 89%. m.p. 92°C. FTIR (ATR) (cm^{-1}): 3276 (Amide A), 3091 (Amide B), 2964 and 2876 (CH_2), 1650 (Amide I) and 1556 (Amide II).

¹H-NMR (CDCl_3 /TFA, TMS as int. ref., ppm) (Figure 2): 7.48 (s, 1H, CONHCH), 6.41 (s, 1H, CH_2NHCO), 4.11 (s, 2H,

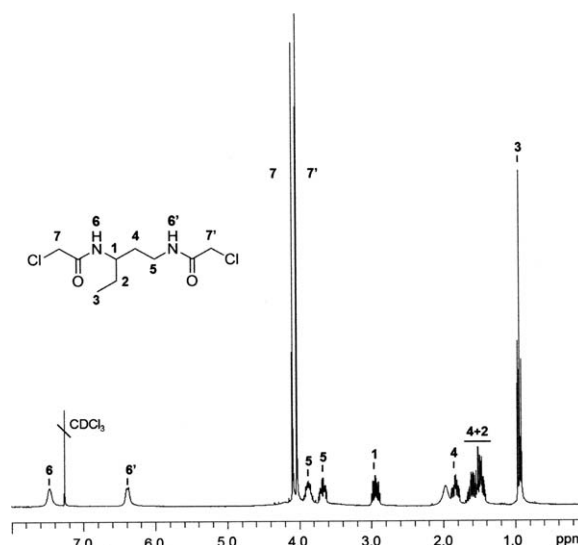


Figure 2. ¹H-NMR spectrum of *N,N'*-bis(chloroacetyl)-1,3-pentanediamine.

ClCH_2CONH), 4.05 (s, 2H, NHCOCH_2Cl), 3.89 and 3.70 (m, 2H, $\text{CH}_2\text{CH}_2\text{NH}$), 2.96 (m, 1H, $\text{NH}(\text{CH})\text{CH}_2$), 1.86 and 1.53 (m, 2H, CHCH_2CH_2), 1.53 and 1.51 (m, 2H, CHCH_2CH_3) and 0.96 (t, 3H, $\text{CH}_3\text{CH}_2\text{CH}$).

N,N'-Bis(chloroacetyl)-1,5-pentanediamine

Yield: 79%. m.p. 122.5°C. FTIR (ATR) cm^{-1} : 3268 (Amide A), 3006 (Amide B), 2929 and 2860 (CH_2), 1633 (Amide I) and 1543 (Amide II).

$^1\text{H-NMR}$ (CDCl_3/TFA , TMS as int. ref., ppm): 6.63 (s, 2H, CONH), 4.04 (s, 4H, ClCH_2CONH), 3.32 (m, 4H, $\text{NHCH}_2\text{CH}_2\text{CH}_2$), 1.58 (m, 4H, $\text{NHCH}_2\text{CH}_2\text{CH}_2$), and 1.37 (m, 2H, $\text{NHCH}_2\text{CH}_2\text{CH}_2$).

Polymerizations

An equimolar mixture of the potassium adipate salt and *N,N'*-bis(chloroacetyl)-1,3-pentanediamine and/or *N,N'*-bis(chloroacetyl)-1,5-pentanediamine was heated at a temperature of 140°C under a nitrogen atmosphere in a reaction tube. After 5 min the mixture liquefied and was then magnetically stirred for a variable period of time (30–360 min). The resulting polymer was next dissolved in formic acid and reprecipitated with ethyl ether (1,3-pentanediamine derivative), methanol (1,5-pentanediamine derivative) or methanol/ethanol mixtures (copolymers).

Samples are abbreviated by indicating the chemical repeat unit sequence (i.e., glc for glycolic acid, 5 for 1,5-pentanediamine, de for 1,3-pentanediamine (DYTEK EP[®]) and 6 for adipic acid). In the case of copolymers, the feed molar fraction of monomer derived from 1,3-pentanediamine with respect to the total amount of pentanediamine derivatives is also specified. Thus, poly(glc-de-glc-co-glc-5-glc 6) 0.25 corresponds to the copolymer prepared from 0.25 moles of *N,N'*-bis(chloroacetyl)-1,3-pentanediamine and 0.75 moles of *N,N'*-bis(chloroacetyl)-1,5-pentanediamine).

Poly(glc-de-glc 6)

Yield: 69%. FTIR (ATR) cm^{-1} : 3283 (Amide A), 3084 (Amide B), 2937 and 2876 (CH_2), 1739 (C=O), 1651 (Amide I) and 1539 (Amide II).

$^1\text{H-NMR}$ (CDCl_3/TFA , TMS as int. ref., ppm) [Figure 6(a)]: 7.40 (s, 1H, NHCO, **6**), 6.38 (s, 1H, NHCO, **6'**), 4.60 (d, 4H, OCH_2CO , **7/7'**), 3.84 and 3.66 (m, 2H, $\text{CHCH}_2\text{CH}_2\text{NH}$, **5**), 2.87 (m, 1H, $\text{NHCHCH}_2\text{CH}_2$, **1**), 2.54 (m, 4H, $\text{OOCCH}_2\text{CH}_2$, **8/8'**), 1.73 (m, 2H, $\text{OOCCH}_2\text{CH}_2$, **9** and 1H, $\text{NHCHCH}_2\text{CH}_2$, **4**), 1.70–1.35 (m, 1H, $\text{NHCHCH}_2\text{CH}_2$, **4** and 2H, CHCH_2CH_3 , **2**) and 0.99 (t, 3H, $\text{CH}_3\text{CH}_2\text{CH}$, **3**).

$^{13}\text{C-NMR}$ (CDCl_3/TFA , TMS as int. ref., ppm) [Figure 6(b)]: 175.9 (CH_2COO , **10/10'**), 171.4 (CH_2CONH , **6/6'**), 63.2 (OCH_2CO , **7**), 50.9 ($\text{NHCHCH}_2\text{CH}_3$, **1**), 37.6 ($\text{NHCHCH}_2\text{CH}_2$, **4**), 33.7 ($\text{CHCH}_2\text{CH}_2\text{NH}$, **5**), 33.5 ($\text{OOCCH}_2\text{CH}_2$, **8**), 27.7 (CHCH_2CH_3 , **2**), 23.9 ($\text{OOCCH}_2\text{CH}_2$, **9**) and 9.6 ($\text{CH}_3\text{CH}_2\text{CH}$, **3**).

Poly(glc-5-glc 6)

Yield: 70% M.p. 79.3°C FTIR (ATR) cm^{-1} : 3270 (Amide A), 3086 (Amide B), 2927 and 2861 (CH_2), 1738 (C=O), 1638 (Amide I) and 1540 (Amide II).

$^1\text{H-NMR}$ (CDCl_3/TFA , TMS as int. ref., ppm): 7.54 (s, 2H, NHCO), 4.60 (s, 4H, OCH_2CO), 3.49 (m, 4H, $\text{CH}_2\text{CH}_2\text{CH}_2\text{NH}$), 2.64 (m, 4H, $\text{OOCCH}_2\text{CH}_2$), 1.80 (m, 4H, $\text{OOCCH}_2\text{CH}_2$), 1.71 (m, 4H, $\text{CH}_2\text{CH}_2\text{CH}_2\text{NH}$) and 1.47 (m, 2H, $\text{CH}_2\text{CH}_2\text{CH}_2\text{NH}$).

$^{13}\text{C-NMR}$ (CDCl_3/TFA , TMS as int. ref., ppm): 175.8 (CH_2COO), 171.4 (CH_2CONH), 62.9 (OCH_2CO), 40.9 ($\text{CH}_2\text{CH}_2\text{CH}_2\text{NH}$), 33.5 ($\text{OOCCH}_2\text{CH}_2$), 28.3 ($\text{CH}_2\text{CH}_2\text{CH}_2\text{NH}$), 23.9 ($\text{OOCCH}_2\text{CH}_2$), and 23.8 ($\text{CH}_2\text{CH}_2\text{CH}_2\text{NH}$).

Measurements

$^1\text{H-NMR}$ spectra were recorded with a Bruker AMX-300 spectrometer operating at 300.1 MHz. Chemical shifts were calibrated using tetramethylsilane as the internal standard and CDCl_3 as the solvent ($\delta(^1\text{H}) = 7.26$ ppm).

Infrared absorption spectra were recorded with a Fourier Transform FTIR 4100 Jasco spectrometer in a 4000–600 cm^{-1} range. A Specac-Teknokroma model Golden Gate attenuated total reflection (ATR) set-up with a heated Single Reflection Diamond ATR Top Plate was also employed.

Molecular weights and polydispersity index (PDI) were estimated by size exclusion chromatography (SEC) using a liquid chromatograph (Shimadzu, model LC-8A) equipped with an Empower computer program (Waters). A PL HFIP gel column (Polymer Lab) and a refractive index detector (Shimadzu RID-10A) were employed. The polymer was dissolved and eluted in 1,1,1,3,3,3-hexafluoroisopropanol at a flow rate of 0.5 mL/min (injected volume 100 μL , sample concentration 1.5 mg/mL). The number and weight average molecular weights were calculated using polymethyl methacrylate standards.

Calorimetric data were obtained by differential scanning calorimetry with a TA Instruments Q100 series equipped with a refrigerated cooling system (RCS). Experiments were conducted under a flow of dry nitrogen with a sample weight of ~ 10 mg while calibration was performed with indium. Heating and cooling runs were carried out at a rate of 20°C/min.

Thermal degradation was studied at a heating rate of 20°C/min with around 10 mg samples in a Q50 thermogravimetric analyzer of TA Instruments and under a flow of dry nitrogen. The analysis was performed in the 25–600°C temperature range.

Samples for enzymatic degradation studies were prepared as thin films by pressing 300 mg of each polymer at room temperature, except poly(glc-5-glc 6), which was heated to 80°C. Due to the sticky nature of samples, pressing was performed between two dialysis films with a pore diameter of 3500 Da to make samples manageable and allow interaction with enzymes and release of degradation products. The resulting films were cut to obtain $1 \times 1 \text{ cm}^2$ plaques of similar weight. Enzymatic studies were carried out with esterase and proteinase media, specifically lipase from *Rhizopus oryzae* and proteinase K from *Tritirachium album*. All plaque samples were exposed to 5 mL of an enzymatic medium based on a saline phosphate buffer (pH 7.4) containing sodium azide [0.02% (w/v)] to prevent microorganism attack and calcium chloride (5 mM) as a cofactor. Incubation was performed in an orbital shaker (60 rpm) at 37°C.

A specific concentration was used for each enzyme: 1000 U/mL for the lipase and 6 U/mL for the proteinase K. The enzymatic solutions were renewed every 72 h due to enzymatic activity loss. Plaque samples were washed with Milli-Q water (Millipore) and dried in an oven at 40°C for 3 h to determine their dry weight. They were subsequently used to continue with the enzymatic degradation study. All experiments were conducted on three replicate samples of each product. Two replicates were used as controls (i.e., samples exposed to media without enzymes) to evaluate possible hydrolytic degradation.

RESULTS AND DISCUSSION

Synthesis of Copolymers

Figure 3(a) shows the DSC heating run of an equimolar mixture of *N,N'*-bis(chloroacetyl)-1,5-pentanediamine and potassium adipate where a well-defined exothermic peak indicative of the polymerization process can be envisaged. The peak temperature is observed at 227°C although the process seems to start at a much lower temperature, close to 140°C. The heating trace also shows an endothermic peak at 121°C which is associated with the fusion of the monomer derived from 1,5-pentanediamine. It is clear that polymerization was initiated after the melting of this monomer and was able to progress even if the potassium adipate salt remained in the solid state.

A similar behavior was observed during the heating run of an equimolar mixture of *N,N'*-bis(chloroacetyl)-1,3-pentanediamine and potassium adipate [Figure 4(a)]. Note that the polymerization peak, start of polymerization and even polymerization enthalpy were highly similar to those found for polymerization of the 1,5-pentanediamine derivative. The main difference corresponds to the melting peak of *N,N'*-bis(chloroacetyl)-1,3-pentanediamine, which had a lower melting enthalpy, appeared at a lower temperature and was so broad that even two peaks were envisaged.

Calorimetric data suggest that both polymerizations could be performed at a similar temperature, which was initially determined at 140°C (i.e. when the exothermic peak started to appear in the DSC analysis), to minimize competitive thermal degradation.

FTIR spectroscopy is an ideal technique to follow the polymerization process by determining the absorbance evolution of the band (1745–1735 cm⁻¹) assigned to the new ester bond formed during the polycondensation process performed at a given temperature, as shown in the insets of Figures 3(b) and 4(b). Thus, a relative conversion degree [$\alpha(t)$] can be evaluated for a given reaction time as

$$\alpha(t) = [A_t - A_0] / [A_\infty - A_0] \quad (1)$$

where A_t is the absorbance at time t , and A_∞ and A_0 are, respectively, the final and initial absorbances.

Both *N,N'*-bis(chloroacetyl)-1,3-pentanediamine and *N,N'*-bis(chloroacetyl)-1,5-pentanediamine monomers and the potassium adipate salt had comparable reactivity at 140°C, as deduced from the similar conversion profiles in Figures 3(b) and 4(b). Thus, 50 and 100% conversions were attained after 30–35 min and around 210 min, respectively. It is clear that

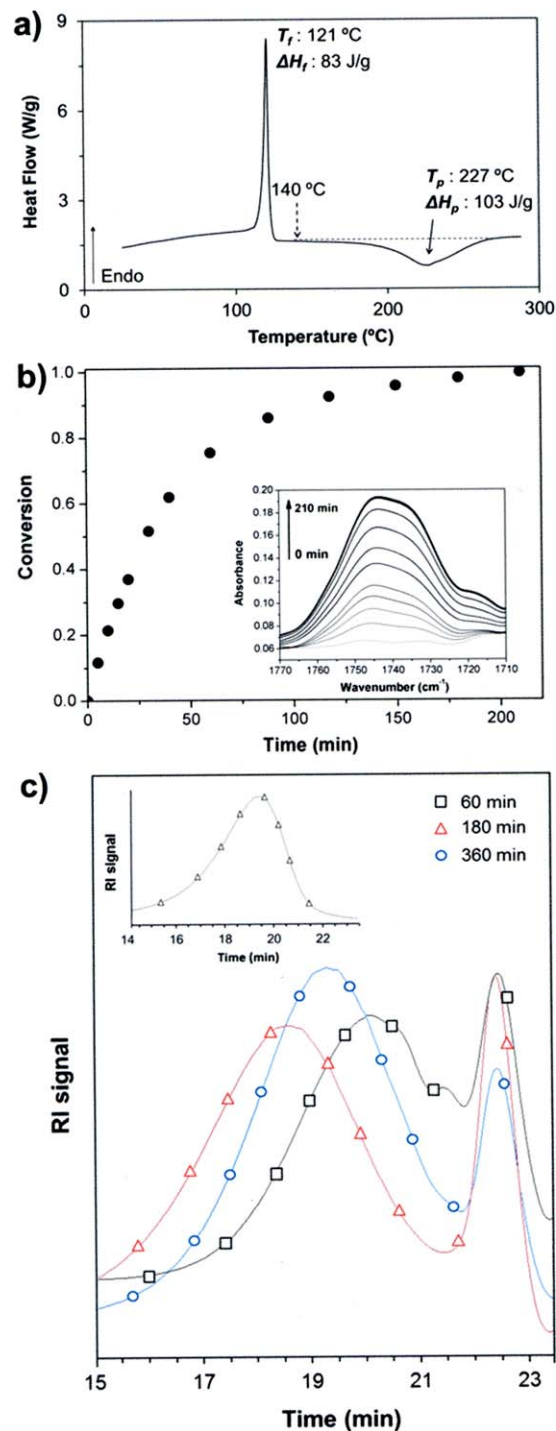


Figure 3. (a) DSC heating run (20°C/min) of a mixture of *N,N'*-bis(chloroacetyl)-1,5-pentanediamine and potassium adipate. (b) Plot of conversion deduced from evolution of the ester absorption band (inset) during isothermal bulk polymerization of a mixture of *N,N'*-bis(chloroacetyl)-1,5-pentanediamine and potassium adipate at 140°C. (c) GPC chromatograms of *N,N'*-bis(chloroacetyl)-1,5-pentanediamine and potassium adipate bulk polymerized samples for the indicated times at a temperature of 140°C. Inset corresponds to the chromatogram of the sample reprecipitated after 360 min reaction at 140°C. [Color figure can be viewed in the online issue, which is available at wileyonlinelibrary.com.]

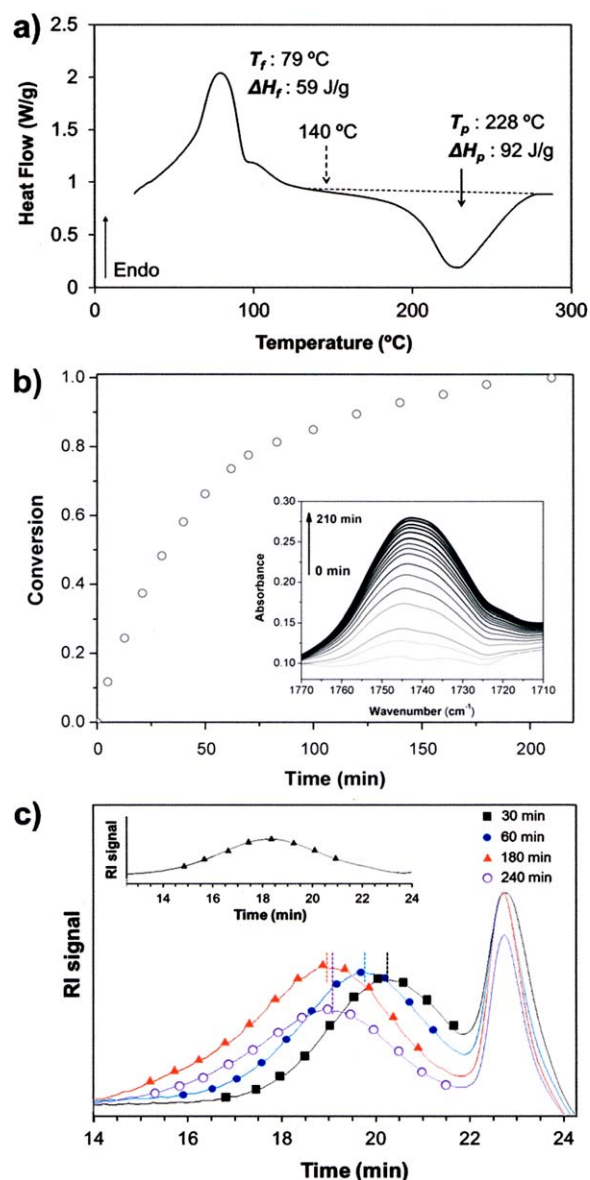


Figure 4. (a) DSC heating run ($20^{\circ}\text{C}/\text{min}$) of a mixture of N,N' -bis(chloroacetyl)-1,3-pentanediamine and potassium adipate. (b) Plot of conversion deduced from evolution of the ester absorption band (inset) during isothermal bulk polymerization of a mixture of N,N' -bis(chloroacetyl)-1,3-pentanediamine and potassium adipate at 140°C . (c) GPC chromatograms of N,N' -bis(chloroacetyl)-1,3-pentanediamine and potassium adipate bulk polymerized samples for the indicated times at a temperature of 140°C . Inset corresponds to the chromatogram of the sample reprecipitated after 180 min reaction at 140°C . [Color figure can be viewed in the online issue, which is available at wileyonlinelibrary.com.]

copolymerization can be effective at this temperature due to the similar reactivity of both diamine derivatives.

The effect of polymerization time on molecular weight was analyzed by GPC taking aliquots of the reaction medium at different times. Typical chromatograms showed a narrow peak at high retention times corresponding to low molecular weight products that remained in the reaction medium and a broad peak associated with the polymer sample. Figure 3(c) is the

chromatograms of the polymerization of N,N' -bis(chloroacetyl)-1,5-pentanediamine. Note that the broader peak shifts to higher molecular weights by increasing the reaction time but after 6 h thermal degradation reactions become significant and the molecular weight decreases. Logically, after purification by reprecipitation the GPC chromatogram shows a broad peak distribution only [inset of Figure 3(c)] due to the removal of all low molecular weight molecules. For the sake of completeness, Figure 4(c) illustrates the time evolution of GPC curves for the polymerization of N,N' -bis(chloroacetyl)-1,3-pentanediamine. The shift of the GPC curve to higher retention times after only 4 h reaction suggests that lower thermal stability is reached. Figure 5 presents the molecular weight data obtained during polymerization of copolymers at 140°C . Some points are worth mentioning:

1. Molecular weight versus reaction time curves always show a maximum due to the occurrence of polycondensation (favored by short reaction times) and thermal degradation reactions (favored by long reaction times).
2. The 1,3-pentanediamine derivatives seem less thermally stable, probably because of the ethyl lateral group. Thus, the reaction time associated with the maximum shifts to lower times with increasing ratios of the N,N' -bis(chloroacetyl)-1,3-pentanediamine monomer in the reaction medium (e.g. 3 h and 5 h for poly(glc-de-glc 6) and poly(glc-5-glc 6) samples, respectively).
3. Molecular weight tends to increase at a slower rate for higher ratios of the N,N' -bis(chloroacetyl)-1,5-pentanediamine monomer in the reaction medium. This seems to be in contradiction with the similar reactivity determined by FTIR analysis but it should also be remembered that GPC data correspond to samples obtained under agitation and in a laboratory scale, which results in significant differences in molecular mobility.

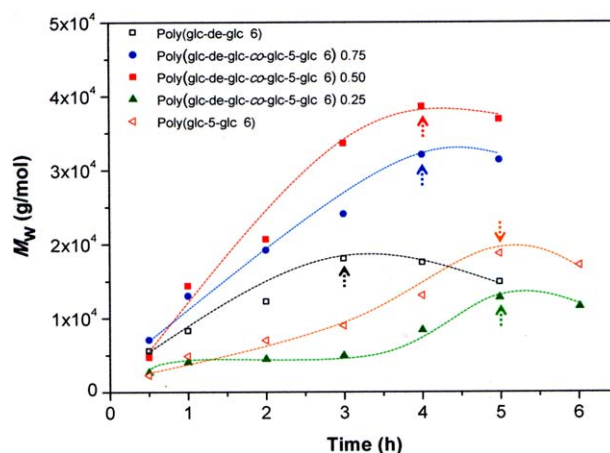


Figure 5. Variation of the weight average molecular weight with reaction time for isothermal bulk polymerization of potassium adipate and different mixtures of N,N' -bis(chloroacetyl)-1,3-pentanediamine and N,N' -bis(chloroacetyl)-1,5-pentanediamine at 140°C . [Color figure can be viewed in the online issue, which is available at wileyonlinelibrary.com.]

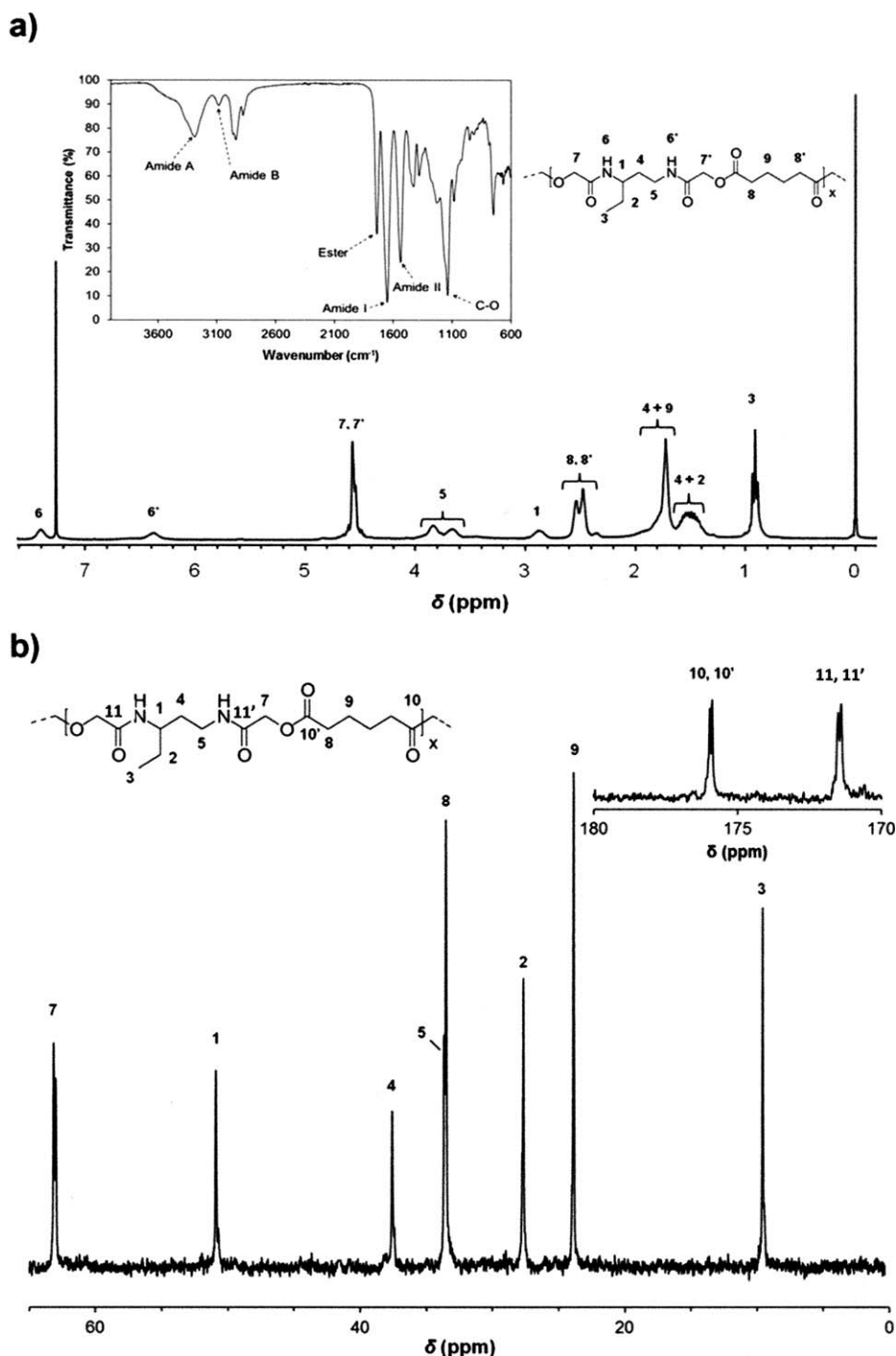


Figure 6. ¹H-NMR (a) and ¹³C-NMR (b) spectra of poly(glc-de-glc 6) showing the assignation of main signals. Insets in (a) and (b) correspond to the FTIR spectrum and the carbonyl NMR signals, respectively.

Table I summarizes the polymerization conditions and main characteristics of all samples after reprecipitation. Polymerization yields were always reasonable and varied in a narrow range (64–70%) whereas molecular weight dispersity was slightly higher (between 2.3 and 2.8).

FTIR spectra of all polymers showed the typical bands of ester and amide groups whereas ¹H-NMR and ¹³C-NMR spectra

were fully consistent with the expected chemical constitution, as shown in Figure 6 for the representative poly(glc-de-glc 6) sample. Note that the proton spectrum was very complicated due to the asymmetric substitution in the diamine unit and the presence of diastereotopic protons [e.g., those labeled 4 and 5 in Figure 6(a)], which are also observed in the spectra of the corresponding monomer (Figure 2). In addition, the methylene protons vicinal to the carboxyl group of the adipic acid unit

Table I. Synthesis and Basic Characterization Data of Poly(glc-de-glc-co-glc-5-glc 6) *x* Copolymers Obtained at 140°C

<i>x</i>	Time (h)	Yield (%)	M_w (g/mol)	D^a	x^b	T_g (°C)	T_f (°C)	ΔH_f (J/g)
1	3	69	16,000	2.3	1	-23°	-	-
0.75	4	66	33,000	2.4	0.72	-13°	-	-
0.5	4	64	38,000	2.6	0.44	-5°	-	-
0.25	5	67	15,000	2.8	0.24	-25 ^d	76	14
0	5	70	18,000	2.4	0	-3 ^d ; 23°	99	62

^aMolecular weight dispersity index determined from GPC.

^bExperimental ratio determined from ¹H-NMR spectra.

^cFrom amorphous samples. In the case of *x* = 0 corresponds to the heating run of a previously melted sample.

^dFrom as-synthesized semicrystalline samples.

seem sensitive to the arrangement of the next diamine unit. However, the ¹³C-NMR spectrum was clearer, discarding the presence of relevant signals associated with degraded samples or terminal groups.

¹H-NMR spectra of all synthesized samples are compared in Figure 7, which also displays the assignment of the main peaks. The gradual diminution of the methyl proton signal (labeled 3) and the increase of the methylene proton signals labeled 10, 11, and 12 for lower ratios of *N,N'*-bis(chloroacetyl)-1,3-pentanediamine monomer units are worth mentioning. Furthermore, signals corresponding to methylene protons of adipic acid units

become insensitive to neighboring units with increasing monomer ratios. Areas of the methyl protons ($A_{0.99}$) and glycolyl protons ($A_{4.60}$) were used to determine the ratio between the two kinds of diamines incorporated into the polymer chain:

$$x = (A_{0.99}/3)/(A_{4.60}/4) \quad (2)$$

Note that the total diamine content can be evaluated through glycolyl content since monomers always contain two glycolyl units linked to each kind of diamine unit. Experimental values determined from ¹H-NMR spectra were always in close agreement with the feed ratio, as indicated in Table I.

The solubility of samples was highly similar, as summarized in Table II for some common solvents. However, the incorporation of diamine units with lateral groups enhanced the solubility of samples in methanol, which makes them suitable for use as coatings (e.g., for bioabsorbable multifilament sutures).

Thermal Properties

The calorimetric heating run shows that the poly(glc-5-glc 6) sample directly obtained from synthesis (i.e., precipitated from solution) has a semicrystalline character with a relatively high melting enthalpy [Figure 8(a)]. In fact, a degree of crystallinity of 47.8% can be estimated by group contribution theory²⁸ (131.1 J/g is the heat of fusion deduced for a 100% crystalline sample considering 4.0, -2.5, and 2.0 kJ/mol as the contributions of methylene, ester and amide groups, respectively). Although a well-defined melting peak appears at 99°C, a very broad endotherm also starts to appear at 34°C. It seems that

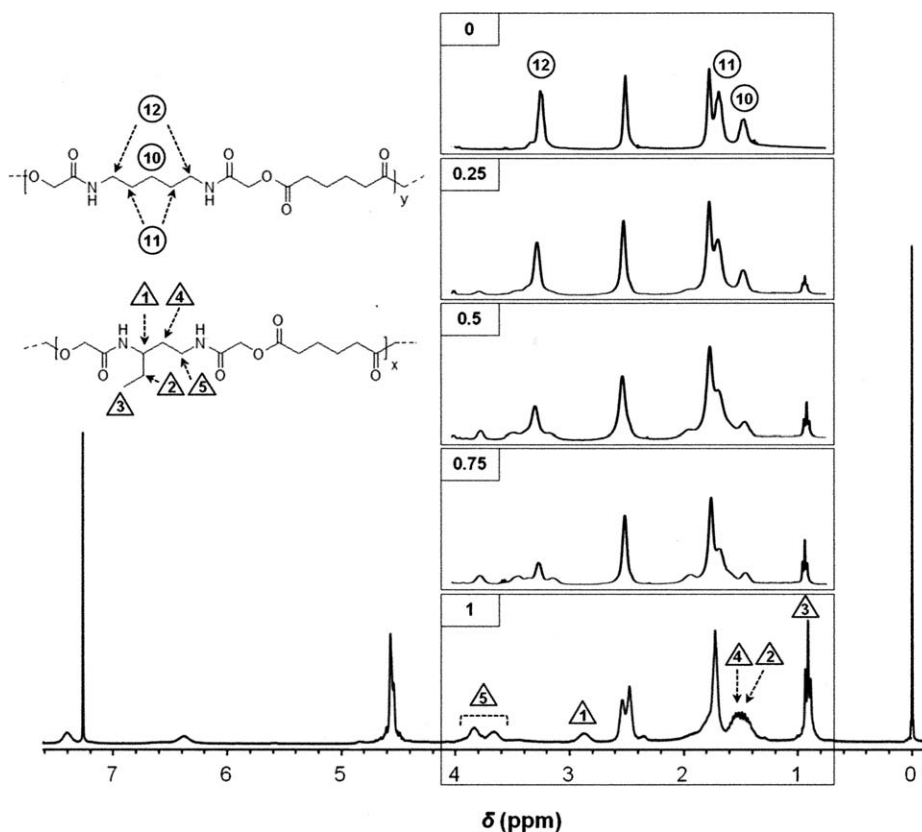
**Figure 7.** ¹H-NMR spectra of all poly(glc-de-glc-co-glc-5-glc 6) *x* synthesized samples.

Table II. Solubility of the Different poly(glc-de-glc-co-glc-5-glc 6) *x* Copolymers in Different Solvents^a

<i>x</i>	MeOH	EtOH	CHCl ₃	THF	Ethyl Acetate	Formic Acid	HFIP
1	++	-	-	+	-	++	++
0.75	++	-	-	+	-	++	++
0.5	++	+	-	+	-	++	++
0.25	++	+	-	+	-	++	++
0	-	+	-	+	+	++	++

^aCode: ++, soluble; + partially soluble (swelling); -, not soluble.

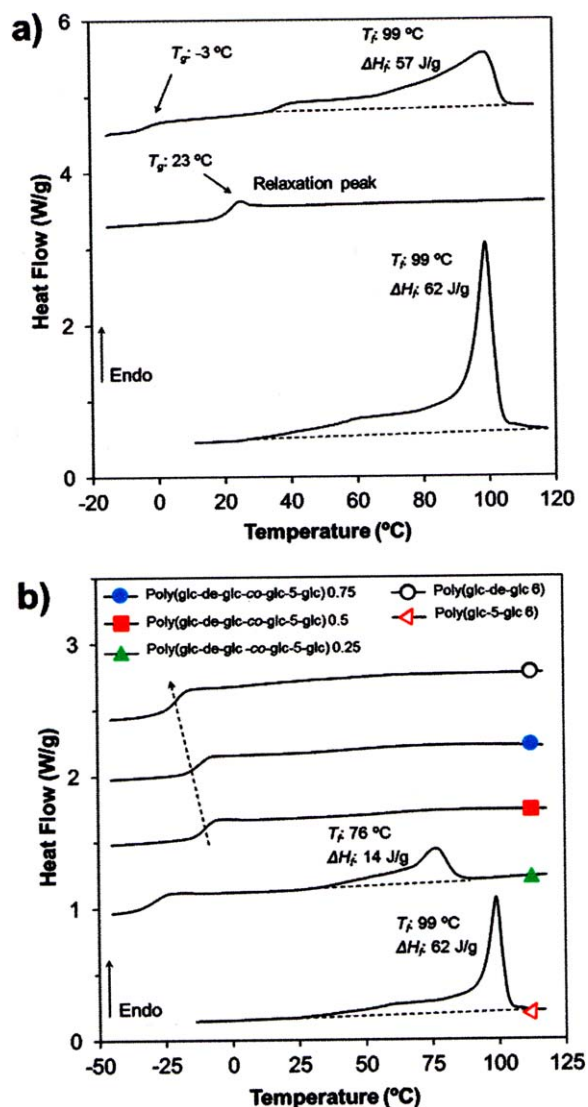


Figure 8. (a) Heating scans performed with the as-synthesized poly(glc-5-glc 6) sample (bottom) after slowly cooling ($10^\circ\text{C}/\text{min}$) to room temperature from the melt state (middle) and drawn film obtained from the molten sample (top). (b) DSC heating traces ($20^\circ\text{C}/\text{min}$) performed with all poly(glc-de-glc-co-glc-5-glc 6) *x* synthesized samples. For the sake of clarity, the trace of poly(glc-5-glc 6) is drawn at a different scale (i.e., the flow rate is twice the value in the ordinate axis). [Color figure can be viewed in the online issue, which is available at wileyonlinelibrary.com.]

thin, highly defective crystals also formed during the precipitation process. Note that the polydispersity index of this sample (Table I) is typical for polycondensation polymers and that the wide melting range cannot be associated with variable polymer molecular weights only. The polymer was not able to hot crystallize during a cooling run from the melt (not shown), even using a low rate (i.e. $2^\circ\text{C}/\text{min}$). The subsequent heating run also indicated that cold crystallization was not feasible [Figure 8(a)]. However, samples were able to hot crystallize when molecular orientation was induced by melt drawing, as shown in the subsequent heating run [Figure 8(a)]. The melting peak was broader than that observed for the solution precipitated sample, although the melting peak temperature was the same. There was a small decrease in crystallinity (43.5%) and the sample had a slightly sticky appearance caused by the small fraction of defective crystals with low melting temperature. This difficulty in crystallizing from the melt or glass state was also previously observed for related poly(ester amide)s derived from the even 1,6-hexanediamine and succinic or adipic acids.²¹ Also interesting is the significant decrease in the melting temperature of the odd diamine derivative compared to the even derivatives (Figure 9). A typical odd-even effect seems to exist despite the available experimental data are limited. Poly(ester amide)s with an even number of carbon atoms in the diamine unit have more symmetrical chemical structures and may give rise to crystal structures with closer packing.

The glass transition temperature of poly(glc-5-glc 6) clearly depends on final crystallinity and specifically increases when the sample becomes completely amorphous [e.g., from -3 to 23°C , as shown in Figures 8(a) and 9]. The more rigid segments seem to be constituted by diamide moieties (e.g. $-\text{CH}_2\text{CONH}(\text{CH}_2)_5\text{NHCOCH}_2-$) are preferentially incorporated into the crystalline phase because of their ability to establish strong hydrogen bonding interactions. In this way, samples with high crystallinity logically showed slightly increased heat capacities

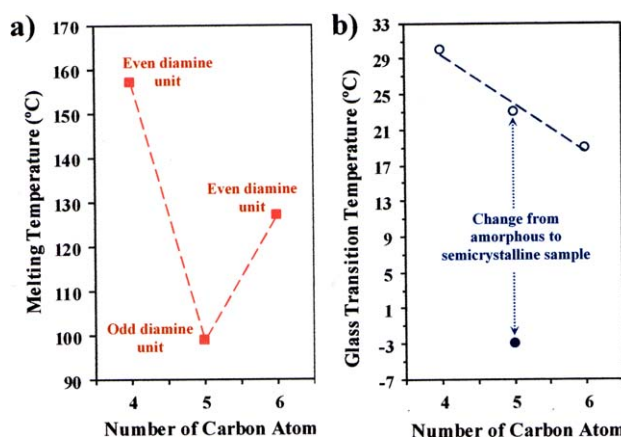


Figure 9. Variation of the melting temperature (a) and the glass transition temperature (b) with the number of carbon atoms of the repeating unit of poly(glc-6-glc 4),²¹ poly(glc-5-glc 6), and poly(glc-6-glc 6)²¹ samples derived from diamines (1,6-hexanediamine or 1,5-diamine), glycolic acid, and dicarboxylic acids (succinic, glutaric, or adipic acids). [Color figure can be viewed in the online issue, which is available at wileyonlinelibrary.com.]

and a transition at a lower temperature due to their higher content of the more flexible diester units (e.g., $-\text{CH}_2\text{OCO}(\text{CH}_2)_4\text{COOCH}_2-$). The DSC heating run of the amorphous sample [Figure 8(a)] also shows an endothermic relaxation peak which is indicative of the trend of the metastable glassy material to achieve equilibrium thermodynamic conditions with lower specific volume, higher stiffness, and lower enthalpy. Finally, it is interesting to note that the glass transition temperature is linearly dependent on methylene content of the repeat unit when comparing fully amorphous samples (i.e., poly(glc-5-glc 6) and samples derived from 1,6-hexanediamine, as shown in Figure 9).

Figure 8(b) also compares the first heating run of all poly(glc-de-glc-co-glc-5-glc 6) x synthesized samples. Only the copolymer with a low 1,3-pentanediamine content ($x = 0.25$) was still able to crystallize from solution, although it was unable to hot crystallize even when molecular orientation was induced. Specifically, a degree of crystallinity of 10.7% was estimated from the melting enthalpy and group contribution data (a heat of fusion of 131.4 J/g is deduced for a 100% crystalline sample when considering a contribution of 4.7 kJ/mol for the CHCH_3 group). The melting peak temperature was clearly lower than that of the homopolymer (i.e., from 99 to 76°C), suggesting the incorporation of some 1,3-pentanediamine units into the crystal structure. Again the peak was very broad, with the fusion of the more defective crystals starting at a temperature close to 30°C. The glass transition temperature decreased for lower 1,3-pentanediamine contents (except for the ester enriched amorphous phase of the sample with $x = 0.25$), suggesting that the ethyl lateral groups had a greater effect on chain mobility than the shortening of the odd diamide unit (i.e., the decrease of the methylene number from 5 to 3 should lead to a slight increase of chain stiffness). Some cautions must be taken into account on this assertion since the synthesized samples have a variation in their molecular weight. Nevertheless, it is significant that the sample without 1,3-pentanediamine units had the higher glass transition temperature and a molecular weight that was clearly lower than determined for other samples having these units [e.g., 18,000 g/mol for poly(glc-5-glc 6) versus 38,000 g/mol for poly(glc-de-glc-co-glc-5-glc 6) 0.5].

X-Ray Diffraction Data and Molecular Arrangement

The complex chemical sequence of poly(ester amide)s makes it almost impossible to perform a detailed analysis of their crystalline structures. Furthermore, structural data based on X-ray and electron diffraction patterns from oriented fibers and single crystals, respectively, are also scarce. However, there are several studies on poly(glc-6-glc 6) (i.e., the related polymer derived from the even 1,6-hexanediamine, glycolic acid, and adipic acid). Thus, a triclinic unit cell with $a = 0.475$ nm, $b = 1.35$ nm, $c = 2.26$ nm, $\alpha = 90^\circ$, $\beta = 77^\circ$, and $\gamma = 64^\circ$ was reported.²¹ Crystalline structure was interpreted in terms of a molecular arrangement with establishment of hydrogen bonds similar to that of polyamides which gave rise to a sheet structure. Specifically, the a parameter corresponds to the typical distance between hydrogen bonded chains (0.475–0.479 nm), and the cell is constituted by three hydrogen-bonded sheets having a shift along the a parameter that accounted for the deduced γ angle. This peculiar packing justified the existence of two strong

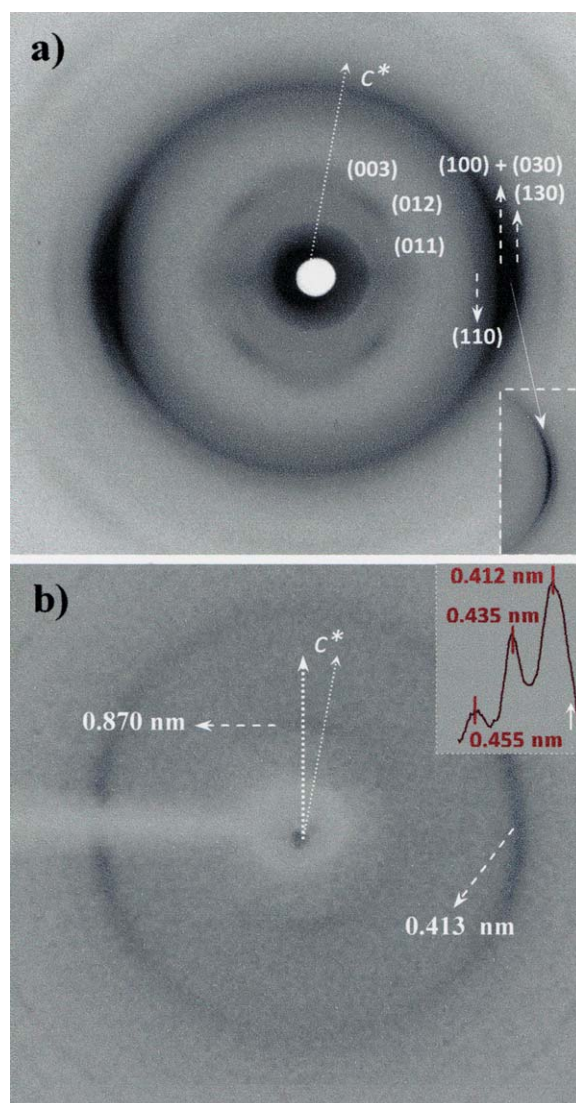


Figure 10. X-ray diffraction patterns of poly(glc-6-glc 6) (a) and poly(glc-5-glc 6) (b) oriented films. Inset in (b) shows the corresponding X-ray diffraction profile (0.470–0.40 nm) of a powder sample directly coming from synthesis. [Color figure can be viewed in the online issue, which is available at wileyonlinelibrary.com.]

equatorial reflections at 0.413 nm and 0.402 nm [Figure 10(a)]. The pattern was also characterized by off meridional reflections ($(00l)$ reflections) which served to determine the β angle and deduce a chain periodicity that became significantly shorter than expected for a fully all-trans conformation (i.e., 2.26 nm as opposed to 2.45 nm).

The X-ray diffraction pattern of poly(glc-5-glc 6) oriented films showed poor orientation and few and broad reflections [Figure 10(b)], showing the difficulty of the sample to crystallize from the melt. However, a strong reflection with an equatorial orientation was observed at 0.413 nm. This single equatorial reflection may suggest a pseudohexagonal packing since this spacing (equal to 0.479 nm \times $\cos 60^\circ$) is characteristic of polyamides with a pseudohexagonal arrangement of hydrogen bonded chains (i.e., the γ -form observed in odd-odd nylons^{29,30} and even the

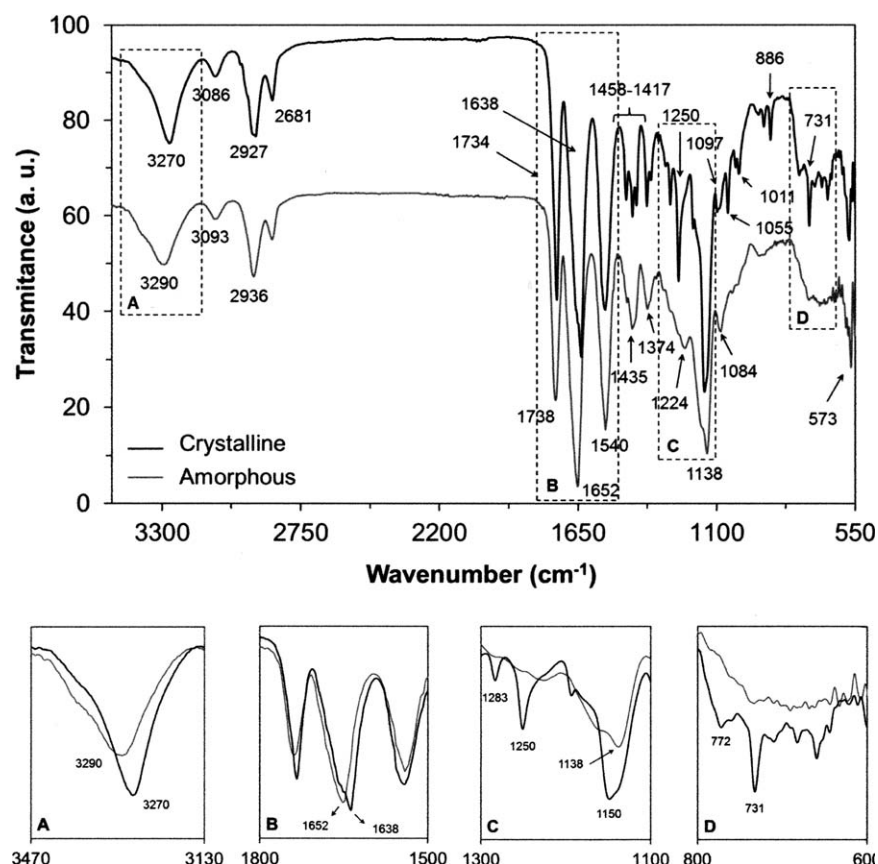


Figure 11. FTIR spectra of semicrystalline and amorphous poly(glc-de-glc 6) samples. Insets show a magnification of the regions with more significant changes.

structure usually obtained at temperatures above the Brill transition^{31–34}. A reflection with a close meridional orientation was observed at 0.870 nm and indexed as the (004) reflection. This value indicates a chain unit repeat (c) between 3.48 and 3.57 nm when cc^* angles of 90° (i.e., unit cell with $\alpha = \beta = 90^\circ$) and 77° (i.e., unit cell similar to the even diamine derivative with $\alpha = 90^\circ$ and $\beta = 77^\circ$) were respectively assumed. Again, chain periodicity becomes clearly shorter than expected for a fully all-trans molecular conformation (i.e., 3.92 nm). X-ray profiles of the powder sample directly obtained from synthesis showed more and better defined reflections [e.g., inset of Figure 10(b)] which point to a sheet structure similar to that postulated for the even derivative. Note the presence of a new reflection at 0.455 nm and a shoulder (see white arrow) of the main peak that may be related to those indexed as (110) and (130) for the even derivative. A reflection at 0.435 nm indexed as (008) and the (004) reflection at 0.870 nm (not shown in the inset) can also be observed, suggesting that powder and oriented film patterns correspond to the same crystalline structure.

FTIR spectra of the semicrystalline as-synthesized sample and the amorphous one obtained after cooling a molten polymer are compared in Figure 11. Some observations mainly concerning the hydrogen bonding arrangement can be made:

1. Amide A (inset A of Figure 11) and amide B bands shifted from 3270 and 3086 cm^{-1} to 3290 and 3093 cm^{-1} respec-

tively, when the sample became amorphous. This shift to higher frequencies can be related to a weakening of hydrogen bonding interactions.³⁵

2. The amide I band shifted from 1638 cm^{-1} to 1652 cm^{-1} (inset B of Figure 11) when the sample became amorphous. It is interesting to note that the first value is usually attributed to a semicrystalline polyamide with a predominant sheet structure (e.g., α/β -forms [35]) whereas the second is typical of amorphous polyamides.
3. The amide II band was observed at 1540 cm^{-1} , which is also a characteristic value for polyamides with a sheet structure since a shift towards 1560 cm^{-1} is usually reported for the pseudohexagonal γ -form.³⁶

In addition, some methylene (e.g., 2927 cm^{-1}) and ester group (e.g., 1150 cm^{-1} , inset C of Figure 11) bands were also found to be sensitive to molecular arrangement since a shift was detected between the spectra of the two kinds of samples. Finally, some bands were clearly enhanced in the as-synthesized sample (e.g., the 1283, 1250, 772, and 731 cm^{-1} bands in insets C and D of Figure 11), and may therefore be useful in evaluating the crystallinity of samples.

Thermal Degradation

Thermogravimetric analysis (Figure 12) shows that all copolymers start to degrade at a similar temperature (i.e., $T_{d,0}$ is found between 260 and 290°C), which is clearly higher than the

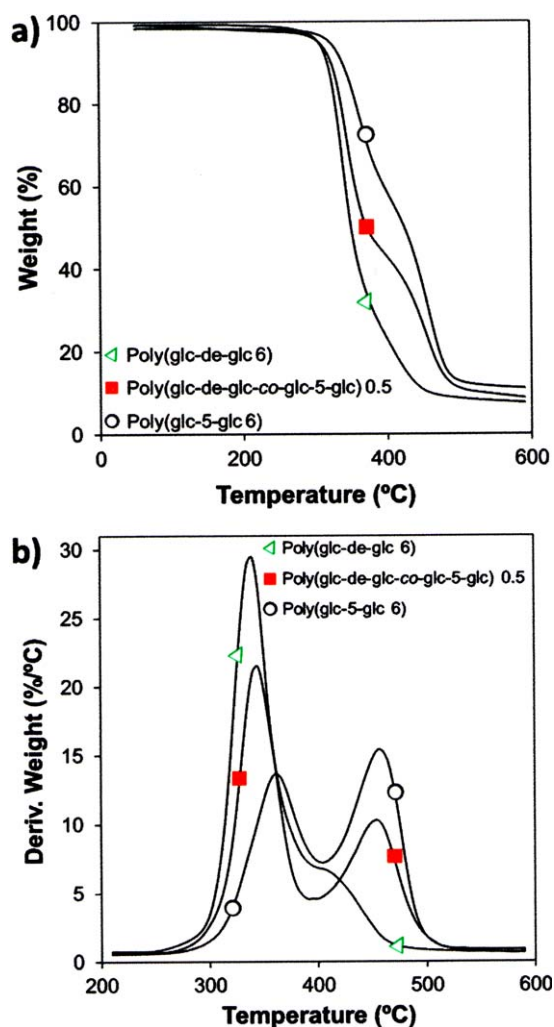


Figure 12. Thermogravimetric (a) and derivative (b) curves for the decomposition of poly(glc-5-glc 6) (○), poly(glc-de-glc-co-glc-5-glc 6) 0.5 (■) and poly(glc-de-glc 6) (◁). [Color figure can be viewed in the online issue, which is available at wileyonlinelibrary.com.]

maximum melting temperature of semicrystalline samples (i.e., 99°C) and obviously higher than the glass transition temperature of amorphous samples. Thus, all synthesized polymers can be thermally processed without problems associated with potential decomposition processes. However, slight differences were observed between the polymers of the studied series since degradation curves were shifted to lower temperatures with decreasing 1,3-pentanediamine content. This can be easily deduced considering that $T_{d,1/2}$ decreased progressively from 426°C to 350°C. It is also worth noting that two degradation steps can be distinguished before reaching a practically constant weight percentage of 15–10% at a temperature higher than 460°C. The first step was generally associated with a decomposition process involving the glycolyl units, as deduced comparing decomposition data obtained from the poly(ester amide) series derived from glycolic acid and ω -amino acids with different methylene length as well as derivatives of glycolic acid, 1,6-hexanediamine and dicarboxylic acids with different methylene length. In both series the weight loss associated with the first step increased with the use

of a shorter ω -amino acid or dicarboxylic acid. In our case, the weight loss associated with the first step increased gradually from 40% to 75% for higher 1,3-pentanediamine contents, suggesting a complex process that could not be rationalized in terms of a simple variation in glycolyl content only since it was constant for all polymers of the series. Probably, the lateral group of the 1,3-pentanediamine unit destabilizes the system and the decomposition of diamide segments constituted by these 1,3-pentanediamine units is also involved in the first degradation step.

Enzymatic Degradation

Degradation was evaluated in enzymatic media with protease and esterase activity. As enzymatic degradation occurs on the sample surfaces only weight losses were determined. Results indicate that all polymers were susceptible to the attack of both enzymes, although degradation was enhanced in the medium containing proteinase K, an enzyme capable of hydrolyzing both amide and ester bonds.³⁷ Furthermore, the choice of enzyme also led to significant differences between the members of the series.

Figure 13(a) clearly shows that rapid weight loss occurred during the first 6 days of exposure to the proteinase K medium and that after this period the degradation rate decreased progressively. Probably, more compact arrangements that hindered enzymatic attack were achieved with decreasing the size of molecular segments. It is also interesting that degradation depended significantly on 1,3-pentanediamine content; specifically, after 21-day exposure the weight loss percentage increased drastically from 41% to 89% with increasing this content from 0% [i.e. poly(glc-5-glc 6)] to 100% [i.e. poly(glc-de-glc 6)]. Copolymers having both diamine units showed intermediate values which logically varied with the 1,3-pentanediamine ratio. Note that all samples were completely amorphous after processing, and had the same amide/ester ratio and even the same methylene content. Thus, changes in degradability could not be explained in terms of sample crystallinity, variation in the number of chemical groups susceptible to degradation or sample hydrophilicity/hydrophobicity. Thus, the presence of ethyl side groups clearly favors proteinase K attack. In fact, and although proteases are primarily considered a protein-degrading enzyme, they have also been proved to be highly specific enzymes that can be seen as extremely important signalling molecules involved in numerous vital processes.³⁸ In some way, ethyl lateral groups may be better recognized by the proteinase K; consequently, breakage of amide links from 1,3-pentanediamine units may become enhanced. It should also be pointed out that degradation of poly(glc-5-glc 6) was found to proceed at a slightly lower rate than that of the previously studied derivative from the even 1,6-hexanediamine [i.e. poly(glc-6-glc 6)].²⁰ In the latter case, a weight loss of 23% was determined for samples synthesized by the same procedure (i.e., with a similar molecular weight) and exposed to the same medium for 24 days. It seems that the higher crystallinity of the even derivative and even its greater hydrophobicity may well account for its slightly lower degradability.

Figure 13(b) shows the different degradation behavior of the series when exposed to a lipase medium. Degradability was

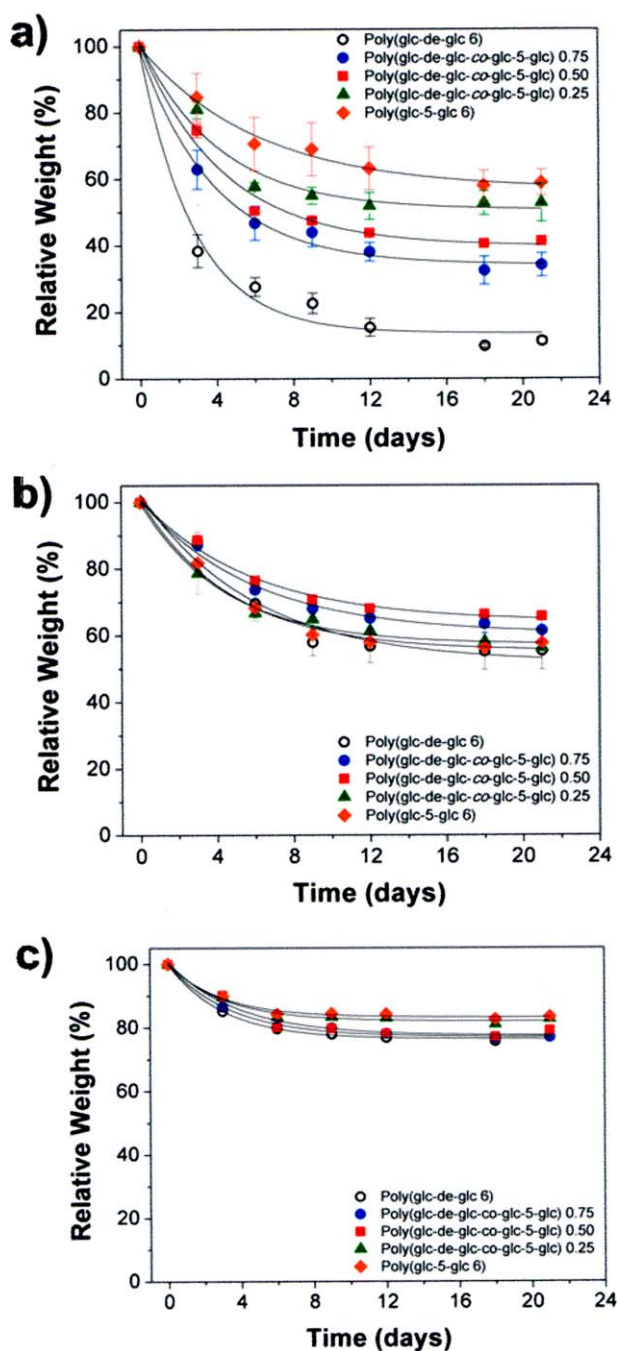


Figure 13. Weight loss percentages of poly(glc-de-glc-co-glc-5-glc 6) *x* samples during exposure to proteinase K from *Tritirachium album* (a), lipase from *Rhizopus oryzae* (b) and PBS (pH 7.2) media at 37°C (c). [Color figure can be viewed in the online issue, which is available at wileyonlinelibrary.com.]

clearly lower than in the case of the proteinase K medium since the weight loss of all polymers was in the 34–45% range after 21-day exposure. Thus, the presence of lateral groups on the diamide moieties did not affect a degradation process that occurs because of breakage of ester bonds. It is also significant that all copolymers of the series have identical diester moieties, and consequently similar degradability should be expected. The

slight differences in the degradation behavior may be due to the different initial molecular weight. Thus, the two homopolymers had a low molecular weight (i.e. M_w : 16,000–18,000 g/mol) and degraded more rapidly, whereas the copolymer with the intermediate composition [i.e., poly(glc-de-glc-co-glc-5-glc 6) 0.5] had the highest molecular weight (i.e., M_w : 37,000 g/mol) and degraded at the slowest rate. Ester group breakages logically rendered few soluble fragments for higher initial sample molecular weight.

For the sake of completeness, hydrolytic degradation under a pH 7.4 buffer at 37°C was evaluated [Figure 13(c)] to make sure that weight losses previously measured were only attributable to enzymatic attack. All samples had similar hydrolytic degradation behavior since differences were not statistically significant. In fact, an average weight loss of 20% was detected after only 8-day exposure, and then the weight remained constant. This suggests that all samples had a small low molecular weight fraction that solubilized easily at the start of exposure by breakage of a reduced number of bonds in each molecular chain. Logically these weight losses should be taken into account if the goal is to evaluate enzymatic degradability only. Note that the exposed trends did not change since hydrolytic weight loss was similar for all samples. However, it should be pointed out that degradation in the lipase medium was greatly affected since a weight loss of 14–25% can only be attributed to enzymatic attack.

CONCLUSIONS

N,N'-bis(chloroacetyl)-1,3-pentanediamine and *N,N'*-bis(chloroacetyl)-1,5-pentane-diamine can be effectively copolymerized with the potassium adipate salt by a thermal polycondensation process with formation of potassium chloride as a driving force. Both diamine monomers showed similar reactivity although different thermal stability, and consequently reaction conditions, had to be carefully selected to avoid competitive thermal degradation reactions.

Incorporation of different ratios of lateral ethyl groups gave rise to a series of copolymers with tuned properties. Specifically, degradability in a protease K enzymatic medium increased for higher contents of 1,3-pentanediamine units. In addition, the incorporation of ethyl groups influenced thermal stability and solubility of copolymers and hindered their crystallization process. In fact, only the 1,5-pentanediamine derivatives were able to crystallize (although with difficulty) from the melt state, leading to poorly oriented films. Hydrogen bonds between amide groups were always established but differences were detected between amorphous and semicrystalline phases. Infrared and preliminary X-ray diffraction data pointed to an arrangement of amide groups similar to that found in the sheet structures of polyamides and a molecular conformation that clearly deviates from a fully all-trans conformation.

The synthesized copoly(ester amide)s, which also derive from glycolic acid units, may be interesting for biomedical applications requiring biodegradability, solubility, and softness.

ACKNOWLEDGMENTS

This research has been supported by grants from MINECO/FEDER and AGAUR (MAT2009-11503, MAT2012-36205, 2009SGR-1208). S.K. M. thanks financial support through a FPI MICINN grant.

REFERENCES

1. Okada, M. *Prog. Polym. Sci.* **2002**, *27*, 87.
2. Lips, P. A. M.; Dijkstra, P. J. *Biodegradable Polymers for Industrial applications*; CRC Press: Boca Raton, **2005**, Chapter. 5, p 198.
3. Rodríguez-Galán, A.; Franco, L.; Puiggali, J. *Polymers* **2011**, *3*, 65.
4. Tokiwa, Y.; Suzuki, T.; Ando, T. *J. Appl. Polym. Sci.* **1979**, *24*, 1701.
5. Guo, K.; Chu, C. C. *J. Biomed. Mater. Res. Part B Appl. Biomater.* **2009**, *89*, 491.
6. Vera, M.; Puiggali, J.; Coudane, J. *J. Microencapsulation* **2006**, *23*, 686.
7. Qian, Z. Y.; Li, S.; He, Y.; Zhang, H. L.; Liu, X. B. *Colloid Polym. Sci.* **2004**, *282*, 1083.
8. Huang, Y.; Wang, L.; Li, S.; Liu, X.; Lee, K.; Verbeken, E.; van de Werf, F.; de Scheerder, I. *Colloid Polym. Sci.* **2006**, *8*, 210.
9. John, G.; Morita, M. *Macromolecules* **1999**, *32*, 1853.
10. Pang, X.; Chu, C. C. *Polymer* **2010**, *51*, 4200.
11. Feng, Y.; Behl, M.; Kelch, S.; Lendlein, A. *Macromol. Biosci.* **2009**, *9*, 45.
12. Ohya, Y.; Toyohara, M.; Sasakawa, M.; Arimura, H.; Ouchi, T. *Macromol. Biosci.* **2005**, *5*, 273.
13. Krook, M.; Albertsson, A. C.; Gedde, U. W.; Hedenqvist, M. S. *Polym. Eng. Sci.* **2002**, *42*, 1238.
14. Liu, X.; Zou, Y.; Cao, G.; Luo, D. *Mater. Lett.* **2007**, *61*, 4216.
15. Morales, L.; Franco, L.; Casas, M. T.; Puiggali, J. *J. Polym. Sci. Part A: Polym. Chem.* **2009**, *47*, 3616.
16. Chen, X.; Zhong, H.; Jia, L.; Ling, J.; Tang, R.; Qiao, J.; Zhang, Z. *J. App. Polym. Sci.* **2001**, *81*, 2696.
17. Barrows, T. H. (Minnesota Mining & Mfg Co). U.S. Patent 4,529,792, (1985).
18. Barrows, T. H. In *Biomedical Polymers: Designed to Degrade Systems*; Shalaby, S. W. Eds.; Hanser Publishers: Munich, Vienna, New York, **1994**; p 97.
19. Vera, M.; Rodríguez-Galan, A.; Puiggali, J. *Macromol. Rapid Comm.* **2004**, *25*, 812.
20. Vera, M.; Admetlla, M.; Rodríguez-Galan, A.; Puiggali, J. *Polym. Degrad. Stab.* **2005**, *89*, 21.
21. Casas, M. T.; Puiggali, J. *J. Polym. Sci. Part B: Polym. Phys.* **2009**, *47*, 194.
22. <http://dytek.invista.com/documents/tds/DYTEK%C2%AE%20EP%20Diamine%20Technical%20Data%20Sheet.pdf>.
23. http://www.ajinomoto.com/about/press/g2012_02_13.html.
24. http://polynerguru.blogspot.com.es/2012_02_01_archive.html.
25. Navarro, E.; Aleman, C.; Subirana, J. A.; Puiggali, J. *Macromolecules* **1996**, *29*, 5406.
26. Puiggali, J.; Franco, L.; Aleman, C.; Subirana, J. A. *Macromolecules* **1998**, *31*, 8540.
27. Morales-Gamez, L.; Soto, D.; Franco, L.; Puiggali, J. *Polymer* **2010**, *51*, 5788.
28. Van Krevelen, D. W.; Nijenhuis, K. In *Properties of Polymers: Their Correlation with Chemical Structure; their Numerical Estimation and Prediction from Additive Group Contributions*. Elsevier: Amsterdam and Oxford, **2009**.
29. Xenopoulos, A.; Clark, E. S. In *Nylon Plastics Handbook*; Kohan, M. I., Ed.; Hanser Publishers: Munich, Vienna, New York, **1995**, Chapter 5, p 108.
30. Kinoshita, Y. *Makromol. Chem.* **1959**, *33*, 1.
31. Brill, R. *Makromol. Chem.* **1956**, *18*, 294.
32. Hirschinger, J.; Miura, H.; Gardner, K. H.; English, A. D. *Macromolecules* **1990**, *23*, 2153.
33. Wendoloski, J. J.; Gardner, K. H.; Hirschinger, J.; Miura, H.; English, A. D. *Science* **1990**, *247*, 431.
34. Ramesh, C.; Keller, A.; Eltink, S. *Polymer* **1994**, *35*, 2483.
35. Skrovanek, D. J.; Painter, P. C.; Coleman, M. M. *Macromolecules* **1986**, *19*, 699.
36. Sibila, J. P.; Sanjeeva, N. S.; Gabriel, M. K.; McDonnell, M. E.; Bray, R. G.; Curran, S. A. In *Nylon Plastics Handbook*; Kohan MI Ed.; Hanser Publishers: Munich, Vienna, New York, **1995**; Chapter 4.
37. Asin, L.; Armelin, E.; Montane, J.; Rodríguez-Galan, A.; Puiggali, J. *J. Polym. Sci. Part A: Polym. Chem.* **2001**, *39*, 4283.
38. Turk, B. *Nat. Rev. Drug Discov.* **2006**, *5*, 785.